

# 1 Introduction

*Asteroids*, also known under the now deprecated name *minor planets*, are a large population of small Solar System bodies which do not display cometary activity. The name asteroid, which was coined by W. Herschel in 1802, is derived from the Greek word for star-like—like stars, and unlike planets or comets, asteroids appear point-like in typical telescopic observations.

Small Solar System bodies are the most pristine material left over from the early days of the Solar System and have undergone much less processing than the planets or the Sun throughout the past 4.6 Gyr. They therefore preserve crucial information on the formation and evolution of the Solar System. Asteroids, in particular, are believed to be remnant building material of the inner planets. Impacts of asteroids and comets have significantly resurfaced the terrestrial planets and their satellites and may have been a significant source of water on Earth (see, e.g., Martin et al., 2006, for a recent review). Meteorites, the remnants of Earth impactors, are the major source of extra-terrestrial material available for laboratory studies; studies of meteorites and asteroids, the parent bodies of most meteorites, benefit considerably from one another. A large impact on Earth could release sufficient energy to cause severe or even fatal damage to our civilization; the Cretaceous-Tertiary extinction event, during which the dinosaurs died out, is widely believed to have been caused by a catastrophic impact.

The increasing public awareness of the impact hazard and general scientific interest has stimulated a dramatic increase in asteroid research over the past decade. This includes the dedication of an increasing number of telescope systems to asteroid discovery.

Nevertheless, the steep increase in asteroid discoveries far outpaces efforts to increase our knowledge about their physical properties.

## 1 Introduction

**Table 1.1:** Overview of asteroids studied by spacecraft, including future targets of Rosetta (launched in 2004) but not including the two rendezvous targets of Dawn (to be launched in June 2007).

Spacecraft	Year	Asteroid target	
Galileo	1991	(951) Gaspra	Flyby
	1993	(243) Ida + Dactyl	Flyby
NEAR–Shoemaker	1997	(253) Mathilde	Flyby
	1998	(433) Eros	Flyby
	2000	”	Rendezvous; landed
Deep Space 1	1999	(9969) Braille	Flyby
Cassini	2000	(2685) Masursky	Distant flyby
Stardust	2002	(5535) Annefrank	Flyby
Hayabusa	2005	(25143) Itokawa	Rendezvous; samples taken (?)
New Horizons	2006	(132524) APL	Distant flyby
Rosetta	2008	(2867) Šteins	Flyby
	2010	(21) Lutetia	Flyby

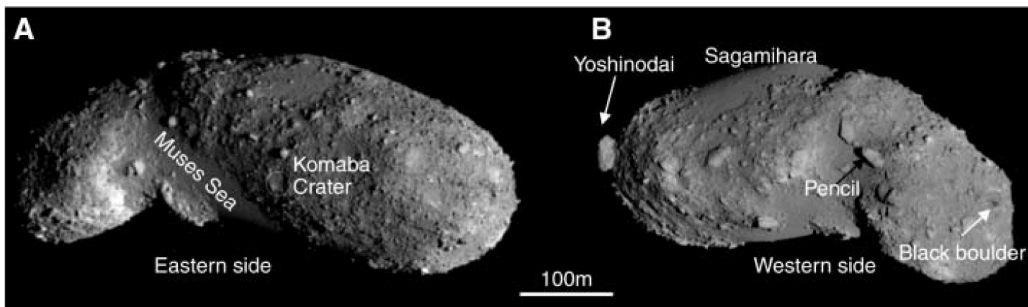


**Figure 1.1:** Global images of near-Earth asteroid Itokawa recorded from the Hayabusa spacecraft. Note the scale! (Figure from Saito et al., 2006)

### 1.1 Space missions to asteroids

Since 1991, when the Galileo spacecraft flew by the asteroid (951) Gaspra, asteroids have been targeted by spacecraft several times, see table 1.1 (see also Farquhar et al., 2002, for a slightly outdated review).

Spectacular insights were gained from results of the asteroid rendezvous missions NEAR-Shoemaker and Hayabusa. NEAR-Shoemaker orbited the near-Earth asteroid (433) Eros for about a year until it successfully soft-landed in February 2001, taking further data from ground. Hayabusa hovered within kilometers from the small (effective diameter around 320 m) near-Earth asteroid (25143) Itokawa for several months in 2005—note that stable spacecraft orbits around such a low-

gravity target are hard to find. After intensively studying the asteroid (see, e.g., Fig. 1.1), Hayabusa touched down on the surface twice to take samples of surface material. Unfortunately, the spacecraft is experiencing technical difficulties and it is unclear whether samples have been taken. Hayabusa is scheduled to return the sample container to Earth in 2010. First Hayabusa results were published in a special issue of *Science* on 2 June 2006 (Vol. 312, issue 5778).

Asteroid missions are currently being planned at all major space agencies:

**Dawn** is a NASA mission to rendezvous with the two large main-belt objects (1) Ceres and (4) Vesta, scheduled for launch in June 2007, arrival at Vesta in 2011 and at Ceres in 2015. Italian and German institutes (including DLR Berlin) contribute two science instruments (Russel et al., 2006).

**Don Quijote** is an ESA mission to produce a measurable deflection of a near-Earth asteroid. The mission will consist of two spacecraft, a kinetic impactor and an orbiter which will intensively study the asteroid before and after the deflecting impact. Don Quijote is currently under phase-A study (Harris et al., 2006).

**Hayabusa 2** is basically a clone of Hayabusa by the Japan Aerospace Exploration Agency JAXA. Hayabusa 2 is planned to be launched in 2010 or 2011 and to return samples from another near-Earth asteroid. An improved version, named Hayabusa Mark 2, is also being planned (Yoshikawa et al., 2006).

**OSIRIS** is a sample-return mission to a near-Earth asteroid currently under consideration at NASA.<sup>1</sup> If selected for further development, the mission may be launched in 2011.

Spacecraft studies of asteroids benefit significantly from ground-based studies of their targets, and vice-versa. Mission planning, in particular, is severely hampered by the general lack of information on the physical properties of potential targets. *Physical studies of potential spacecraft target asteroids are of crucial importance in this respect.*

---

<sup>1</sup> See <http://www.nasa.gov/centers/goddard/news/topstory/2007/osiris.html>. OSIRIS is not to be confused with the telescope instruments of the same name, which are located on board the Rosetta spacecraft, at the Keck II telescope, and at the Gran Telescopio Canarias, respectively.

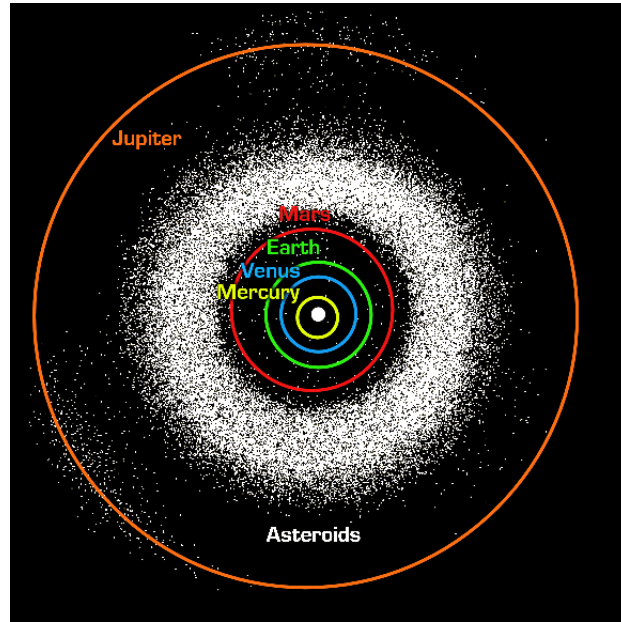


**Figure 1.2:** Asteroids in the inner Solar System out to Jupiter. Note the presence of some asteroids close to the terrestrial planets. Figure credit: NASA/JPL-Caltech/R. Hurt (SSC-Caltech).

## 1.2 Asteroid populations and their origins

Since 1 Jan 1801, when Piazzi discovered (1) Ceres,<sup>2</sup> the number of known asteroids has increased dramatically. As of 2 May 2007, 374,256 asteroids are known, 157,788 of them have well-established orbits (see <http://cfa-www.harvard.edu/iau/lists/ArchiveStatistics.html>). Both numbers are increasing by the thousands per month due mostly to dedicated asteroid discovery programs. New telescope systems, which are currently being built (such as Pan-STARRS, see Kaiser et al., 2002), are expected to result in a further increase of the asteroid discovery rate.

As can be seen from Fig. 1.2, there are three main asteroid populations in the inner Solar System:<sup>3</sup>

**Main-belt asteroids (MBAs)** Most known asteroids orbit the Sun in the region between the orbits of Mars and Jupiter, called the asteroid belt or main

<sup>2</sup> Ceres has been reclassified as a dwarf planet at the IAU General Assembly in August 2006.

<sup>3</sup> While small bodies beyond Jupiter's orbit without cometary activity, such as Centaurs or trans-Neptunian objects, are given asteroid designations, we shall not consider them as asteroids in the following. They are probably very rich in volatiles and resemble comets more closely than asteroids.

belt. The accretion process in the main belt stopped before a planet could be formed, probably due to dynamical excitation through the gravity of forming Jupiter; present MBA encounter velocities are so high that collisions are more likely to produce fragmentation than accretion (Petit et al., 2002). MBAs are thus remnant planet building material, left-overs from the formation of the Solar System which have undergone only limited processing in the past 4.6 Gyr.

The largest main-belt object is (1) Ceres with a diameter around 950 km. The observed asteroid size-frequency distribution increases steeply with decreasing size, but drops towards small sizes due to observational incompleteness (in other words: the smallest asteroids have not been discovered, yet). The smallest newly-discovered MBAs are typically a few km in diameter.

**Near-Earth asteroids (NEAs)** Since the discovery of (433) Eros in 1898 it is known that there is an intriguing population of asteroids which approach Earth. The Earth-like orbits of some NEAs make them accessible for spacecraft with only a moderate amount of propellant and thus at a relatively low cost.

On average, NEAs are significantly smaller than the known MBAs; the largest NEA is (1036) Ganymede with an estimated diameter around 32 km, objects as small as a few tens of meters have been detected. As of 1 May 2007, 4619 NEAs have been discovered, including 712 objects with an estimated diameter of 1 km or larger.<sup>4</sup> The total number of the latter is estimated to lie between 700 and 1,100 (Werner et al., 2002; Stuart and Binzel, 2004).

A particularly noteworthy group of NEAs are the Potentially Hazardous Asteroids (PHAs), which approach Earth's orbit to within 0.05 AU and have diameters above 150 m.<sup>5</sup> As of 7 May 2007, 860 PHAs are known.

**Jupiter Trojans** There are two large asteroid groups beyond the main belt, collectively referred to as Jupiter Trojans. They are in stable 1:1 resonance with Jupiter, librating around the  $L_4$  and  $L_5$  Lagrange points which lead and trail the planet by  $60^\circ$  in heliocentric ecliptic longitude, respectively.

---

<sup>4</sup> Source: <http://neo.jpl.nasa.gov/stats/>. Note that the number of objects above 1 km in diameter depends on the assumed albedo—see also sect. 1.5.1.

<sup>5</sup> Note that the diameter of most NEAs is unknown; technically, PHAs are therefore defined as having an absolute optical magnitude  $H$  (see sect. 1.5.1) below 22, which corresponds to a diameter above 150 m for an assumed geometric albedo of  $p_V = 0.13$ .

## 1 Introduction

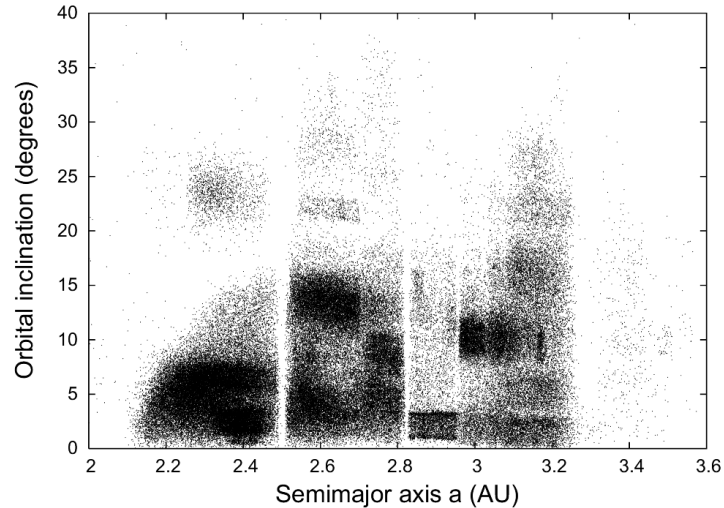


**Figure 1.3:** Scatter plot of the orbital parameters of numbered MBAs. The Kirkwood gaps are clearly seen, e.g. at semimajor axes of  $a \sim 2.5$  AU (3:1 mean-motion resonance with Jupiter), at some 2.8 AU (5:2 resonance), roughly 2.96 AU (7:3 resonance), and the sharp boundary shortward of 3.3 AU (2:1 resonance). Also some significant clusters corresponding to asteroid families are clearly seen, e.g. the Koronis family situated at low inclinations between the 5:2 and 7:3 resonances, seen as a relatively sharp rectangle. (Orbital parameters were retrieved from the University of Pisa AstDys service, <http://hamilton.dm.unipi.it>, on 8 Jan 2007)

The origin of the Trojans is currently under debate. While they were long believed to have formed near their present position (see, e.g., Marzari et al., 2002), it has been argued by Morbidelli et al. (2005) that their orbital distribution indicates they were captured by Jupiter during the time of the Late Heavy Bombardment, and that they share a volatile-rich parent population with comets and small bodies in the outer Solar System. The latter theory is supported by the rather uniform spectral properties and albedos of Trojans similar to cometary nuclei (Barucci et al., 2002) and with recent physical studies of large Trojans (Marchis et al., 2006; Emery et al., 2006).

Orbits inside the main belt are highly chaotic, mostly due to the gravitational influence of massive and near-by Jupiter. In particular, many main-belt orbits are unstable due to resonance with Jupiter; there is a significant depletion in objects on such orbits, the Kirkwood gaps (Kirkwood, 1869, see also Fig. 1.3).

**Asteroid families** While the largest MBAs are believed to be primordial, most MBAs below a certain threshold size appear to be fragments of larger parent bodies

which underwent a catastrophic collisional disruption (Nesvorný et al., 2006). One might expect fragments of such a breakup event to be on rather similar orbits. Indeed, as can be seen in Fig. 1.3, there are statistically significant clusters in the orbital elements of MBAs referred to as *asteroid families*, which were first noticed and explained by Hirayama (1918) (see Zappalà et al., 2002, for a review). The reflection spectra of asteroids belonging to a family are generally very similar, confirming their common origin (Cellino et al., 2002).

Most known asteroid families appear to be very old, on the order of several 100 Myr (Carruba et al., 2003). Due to chaotic dynamics, asteroid families disperse over timescales of roughly 1 Gyr, making old families hard to detect dynamically (Nesvorný et al., 2002b). The ages of very young families, on the other hand, can be determined directly, by numerically integrating the orbits of family members backward in time until convergence is reached; a spectacular case is that of the Karin cluster, the age of which has been determined by Nesvorný et al. (2002a) to be only  $5.8 \pm 0.2$  Myr. The convergence of this backward integration has been shown to improve significantly if the Yarkovsky effect (see sect. 1.3) is taken into consideration (Nesvorný and Bottke, 2004). Recently, asteroid families even younger than 1 Myr have been reported by Nesvorný and Vokrouhlický (2006).

**The origin of NEAs** It is now widely accepted that the dominant NEA source population is the main belt, followed by extinct cometary nuclei providing  $15 \pm 5$  % of the population (see Binzel and Lupishko, 2006, and references therein). This is consistent with the diversity in spectral properties and albedo observed among NEAs, which is similar to that of MBAs.

The only known means of delivering sufficient numbers of MBAs into near-Earth space is through resonances with Jupiter and later perturbations by the inner planets, which may temporarily trap them in near-Earth orbits, although collisions with the Sun or ejection out of the Solar System are more likely (see, e.g., Morbidelli et al., 2002, and references therein).

The timescale for resonant ejection out of the main belt is a few Myr, the dynamical lifetime of NEAs is on the order of 10 Myr. However, as apparent from the crater record on terrestrial planets and their satellites, the NEA population has been rather stable over the past 4 Gyr (Ivanov et al., 2002; Werner et al., 2002). This suggests a steady effect which continuously replenishes the NEA source regions.

## 1 Introduction

It is now widely believed that this is accomplished by the Yarkovsky effect (see sect. 1.3). The Yarkovsky-induced drift inside the main belt takes much longer than the actual resonance-driven transport into near-Earth space, it is therefore the strength of the Yarkovsky effect that determines the timescale and size-dependent efficiency of NEA delivery (Morbidelli and Vokrouhlický, 2003). This is supported by the observed cosmic-ray exposure ages of meteorites, which average around 10–100 Myr for stony meteorites and an order of magnitude larger for iron meteorites,<sup>6</sup> significantly longer than the NEA dynamical lifetime and indicative of a substantial drift time spent inside the main belt (see, e.g., Bottke et al., 2006, and references therein).

### 1.3 The Yarkovsky and YORP effects

It has been realized over the past decade that asteroid dynamics is governed not only by gravity and mutual collisions, but also by the non-gravitational Yarkovsky and YORP effects, both caused by the recoil force from thermally emitted photons. As with ion spacecraft propulsion, the resulting momentum transfer is slight but steady, and therefore capable of slowly but substantially altering the orbits (Yarkovsky effect) and spin states (YORP effect) of small asteroids or meteoroids.<sup>7</sup> Both effects have been observed (see below). See Bottke et al. (2006) for a recent review.

**Yarkovsky effect** As depicted in Fig. 1.4, surface temperature asymmetries due to thermal inertia (see sect. 1.5.8) lead to a gradual increase or decrease in orbital semimajor axis  $a$ , depending on the spin axis orientation and obliquity. There are diurnal and seasonal components of the Yarkovsky effect, which are respectively most efficient in the situations depicted in Fig. 1.4.

*Since the Yarkovsky effect is driven by surface temperature asymmetries, it depends crucially on the thermal inertia.* Specifically, it vanishes in the limiting cases of zero and infinite thermal inertia where the temperature distribution is

---

<sup>6</sup> Note that the Yarkovsky effect is generally less effective for objects with very high thermal inertia, such as metallic bodies (see sect. 1.3).

<sup>7</sup> Orbital drift due to thermal emission was first considered by Yarkovsky (1901) in a private publication (which was long lost, but has recently been rediscovered; see Brož, 2006, for a reprint). Öpik, having read Yarkovsky’s paper, repropoed and named the Yarkovsky effect much later (Öpik, 1951), but until the 1990s it was widely considered irrelevant. The YORP effect was proposed by Rubincam (2000), and named after Yarkovsky and also O’Keefe, Radzievskii, and Paddack, who had considered similar effects between 1954 and 1976.



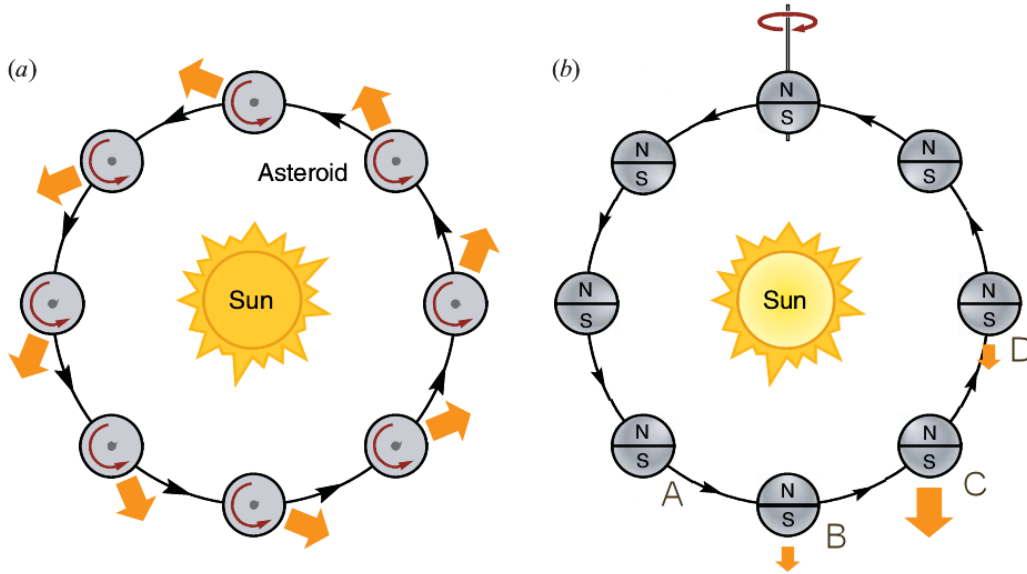


**Figure 1.4:** (a): Schematic depiction of the *diurnal Yarkovsky effect* for a spin axis perpendicular to the orbital plane. Due to thermal inertia, the trailing afternoon side of a prograde rotator is hotter than the leading morning hemisphere, leading to an emission surplus from the former. The resulting net force (arrows) has an accelerating component tangential to the orbit, causing most prominently a secular increase in orbital semimajor axis  $a$  (the radial force component is typically negligible against solar gravity). Analogously, retrograde rotators are decelerated by the Yarkovsky effect, their  $a$  decreases. (b): *Seasonal Yarkovsky effect*, with the spin axis inside the orbital plane. There is an emission surplus from the summer hemisphere. Thermal inertia causes a phase shift between seasons and orbital revolution (orange arrows), leading to a net tangential force component after averaging over one orbit (see positions A–D). The seasonal effect always decreases  $a$ . (Figure adapted from Bottke et al., 2006).

symmetric about the subsolar point. Obviously, spin rate and heliocentric distance are also relevant.

Very importantly, the Yarkovsky effect is size dependent: For objects much larger than the penetration depth of the heat wave (typically at the cm-scale) and all other parameters kept constant, the photon recoil force scales with  $D^2$  (with diameter  $D$ ), while the mass scales with  $D^3$ , so the acceleration scales with  $D^{-1}$ . Smaller objects become increasingly isothermal, weakening the Yarkovsky effect; their interaction with the solar radiation field is dominated by the Poynting-Robertson effect or the radiation pressure.

There is now ample evidence that the Yarkovsky effect strongly influences the orbital dynamics of asteroids below  $\sim 20$  km in diameter:

- The small NEA (6489) Golevka was shown by Chesley et al. (2003) to have

## 1 Introduction

undergone an orbital drift in the years 1991–2003 which cannot be explained by gravitational perturbations alone, but is fully consistent with an additional Yarkovsky-induced drift. The Yarkovsky effect had previously been found to alter the orbit of the LAGEOS satellite (Rubincam, 1987, 1988, 1990).

- As seen above, there must be a steady mechanism bringing small MBAs into powerful resonances which deliver them into near-Earth space—only the Yarkovsky effect is known to do so in a way consistent with the observed NEA distributions in size, spectral type, and spin axis obliquity. In particular, its size dependence explains the apparently different size-frequency distributions of NEAs and MBAs (see Delbo’ et al., 2007a, for a detailed discussion).
- The Yarkovsky effect is required to explain the observed orbital distribution inside asteroid families. Most spectacularly, the orbits of asteroids belonging to the very young Karin family (see above) were seen to have evolved under the Yarkovsky effect (Nesvorný and Bottke, 2004). Furthermore, Yarkovsky-induced drift is required to make the observed orbital dispersion in evolved asteroid families compatible with that of young families and also with model calculations of the initial fragment ejection velocity distribution (Carruba et al., 2003; Bottke et al., 2006).
- The Yarkovsky effect is crucial to assess the impact hazard from individual asteroids. Specifically, it determines whether the NEA 1950 DA, the object with the highest currently known impact probability (see sect. 1.4), will hit Earth in 2880 or not (Giorgini et al., 2002).

**YORP effect** The photon recoil force combined with the radiation pressure of absorbed sunlight may also cause a net torque, altering the spin axis obliquity and the rotation rate of small objects. The YORP torque depends critically on the object’s shape, in particular it vanishes for spherical or ellipsoidal objects (see Scheeres, 2007, for a recent definition of a shape-dependent parameter describing the strength of the YORP torque). While small asteroids are known to have highly irregular shapes in general, the shape of individual objects is usually unknown, although that situation is likely to improve significantly in the next decade (see sect. 1.5.4). The YORP effect is therefore less well studied than the Yarkovsky effect.

Nevertheless, the first direct observations of YORP-induced shifts in rotational period have very recently been reported for the NEAs (1862) Apollo (Kaasalainen et al., 2007) and (54509) YORP (Lowry et al., 2007; Taylor et al., 2007, 54509 was known as 2000 PH5 before 2 April 2007; see also sect. 6.4). The YORP effect was seen by Vokrouhlický et al. (2003) to determine the distribution of spin axis obliquities in asteroid families. The YORP effect may also explain the observed size-dependence of asteroid spin-rate distributions (see sect. 1.5.3) and may be important in the forming of binary asteroid systems (see sect. 1.5.6).

## 1.4 Asteroids impacting Earth: Hazard and link to meteorites

The terrestrial planets and their satellites have been resurfaced by impact cratering. This is quite evident on bodies such as the Moon or Mars, where erosion processes are relatively slow, but also on Earth a significant number of impact craters has been preserved—the most widely known in Germany is the Nördlinger Ries.

Most Earth impactors are very small in size and are completely destroyed upon atmospheric entry causing only a “falling star”. Among objects that reach the ground, the majority is barely large and robust enough to do so—these produce meteorites which represent the major source of extraterrestrial material available for study in Earth laboratories. Large impactors some thousand tons in mass or above, however, are not significantly decelerated by the atmosphere. They hit the ground at velocities above the Earth escape velocity of 11.2 km/s and release their correspondingly large kinetic energy in a crater forming process. While our understanding of the latter is still highly incomplete (see, e.g., Holsapple et al., 2002; de Niem, 2005, and references therein) it is clear that impactors with diameters around 1 km release a significantly higher amount of energy than a nuclear warhead; such impacts would cause global catastrophes (see, e.g., Morrison et al., 2002; Chapman, 2004b, for reviews). The Cretaceous-Tertiary extinction event, during which the dinosaurs died out, is widely believed to have been caused by the impact of an object around 10 km in diameter (Alvarez et al., 1980).

The US Congress held hearings to investigate the impact hazard and charged NASA with the task of discovering 90 % of all near-Earth objects (NEOs) larger than 1 km in diameter within ten years; this *Spaceguard Survey* was initiated in 1998, the due date for the spaceguard goal is end of 2008. Several successful aster-

## 1 Introduction

oid discovery programs have been initiated leading to a steep and ongoing increase in asteroid discoveries. A follow-up discovery program, possibly requiring NASA to discover 90 % of all NEOs above 140 m in diameter until 2020, is currently under discussion.<sup>8</sup> It might include the deployment of mid-infrared space telescopes for asteroid discovery, such as the proposed NASA mission NEOCam (Mainzer et al., 2006).

As of 7 May 2007, the highest known Earth impact probability for an individual object is 0.33 % for a potential impact of the 1.1 km wide NEA (29075) 1950 DA in 2880 (Giorgini et al., 2002)—the only known impact probability larger than the accumulated background risk due to unknown objects of comparable size, thus leading to a positive hazard rating on the Palermo scale by Chesley et al. (2002). It is worth pointing out that the uncertainty in the risk assessment by Giorgini et al. is dominated by the lack of knowledge of physical properties of the asteroid which govern the magnitude of the Yarkovsky effect.

The NEA (99942) Apophis (then known as 2004 MN4,  $270 \pm 50$  m in diameter, see Delbo' et al., 2007b) held, for a brief period after its rediscovery in December 2004, an unprecedentedly large probability for an impact in 2029, peaking at 2.7 % and severely disconcerting the NEA community over the Christmas holidays. On 27 Dec 2004 the 2029 impact could be ruled out on the basis of newly obtained astrometric data; the miss distance from the geocenter in 2029 is currently estimated to be  $5.89 \pm 0.35$  Earth radii ( $3\sigma$  uncertainty; Chesley, 2006). The subsequent orbit, however, will be severely perturbed by Earth's gravity, possibly onto impact course. The corresponding risk is dominated by a potential impact in 2036, with a probability of  $2.2 \cdot 10^{-5}$ . Again, for accurate risk assessment the Yarkovsky effect must be taken into consideration (Chesley, 2006).

The design of asteroid deflection missions, which would become necessary if an impactor were to be discovered, is an active area of engineering research (see, e.g., Kahle et al., 2006). ESA is planning a precursor mission to an asteroid deflection mission, *Don Quixote*, which is currently under phase-A study (see sect. 1.1).

### 1.5 Physical properties of asteroids

There is a growing body of information on the physical properties of asteroids, although the rapid discovery rate leaves most known objects uncharacterized. Some

---

<sup>8</sup> A law requiring NASA to report to Congress about the feasibility of such a program was signed into law in December 2005, NASA's report to Congress was published in March 2007; see <http://neo.jpl.nasa.gov/neo/report2007.html>.

asteroids, however, have been scrutinized with spacecraft or have been studied by ground-based observers in great detail.

The emerging picture is still rather incomplete and highly diverse.

### 1.5.1 Diameter and albedo

For most asteroids, the size, arguably the most basic physical property, is only poorly known. Note that asteroids are typically far too small to be spatially resolved with current telescopes. In only a few cases could asteroid sizes be determined by means of direct imaging from near-by spacecraft, the Hubble Space Telescope, or ground-based telescopes equipped with adaptive optics. Another rather direct way of determining asteroid sizes is from observations of stellar occultations.

For most asteroids, only optical photometric data are available, typically from astrometric measurements with limited photometric accuracy. The amount of reflected sunlight is proportional to the projected area and the albedo, allowing coarse conclusions on the size to be drawn. An important quantity is the absolute optical magnitude  $H$ , which is defined as the visual magnitude corrected to heliocentric and observer-centric distances of 1 AU and a solar phase angle of  $0^\circ$  (Bowell et al., 1989).  $H$  is related to diameter  $D$  and geometric albedo  $p_V$  by (Fowler and Chillemi, 1992):

$$D = 10^{-H/5} \frac{1329 \text{ km}}{\sqrt{p_V}}. \quad (1.1)$$

Asteroid albedos range from some  $p_V = 0.02$  up to around 0.6, thus diameters estimated in this way are very uncertain.

A widely used method to determine asteroid sizes is from observations of their thermal emission, which is proportional to the projected area but only a weak function of albedo (see chapter 2 for a detailed discussion). This method, pioneered by Allen (1970), is the source of most known asteroid diameters (Tedesco et al., 2002a). Other methods of determining asteroid sizes include observations at radar wavelengths (Ostro et al., 2002).

Alternatively, the diameter can be determined if  $p_V$  is known. Methods for determining asteroid albedos include studies of the optical brightness and also of the polarization of reflected sunlight as a function of solar phase angle (see Muinonen et al., 2002, for a review; note that the latter method is so far based on a purely empirical correlation between albedo and certain polarization properties).

### 1.5.2 Taxonomy

Conclusions on the mineralogical composition of asteroid surfaces can be drawn from reflection properties at visible and near-IR wavelengths, chiefly from spectral features and albedo measurements. Asteroid reflection properties are routinely compared to those of meteorites. This way, much could be learned about the composition of asteroids and about the origin of most meteorites.

Different kinds of taxonomic systems are used in order to describe observed asteroid reflection properties, and also to link them with analogue meteorites. The most widely used taxonomic systems are those by Tholen (1984) and Bus and Binzel (2002). While taxonomic classification relies chiefly on spectroscopic or spectrophotometric observations, it can be greatly constrained with albedo measurements alone.

A large number of taxonomic classes have been proposed, but most asteroids belong to one of the following classes (or “complexes” in the notation of Bus and Binzel, 2002) with generally mnemonic names:

**C** is for carbonaceous: C-type asteroids display spectra and albedos consistent with a composition similar to that of carbonaceous chondritic meteorites. They are very dark, generally  $p_V < 0.1$ . Most objects in the outer main belt appear to be C types (see Bus and Binzel, 2002, Fig. 19).

**S** is for siliceous: S-type asteroids show spectral features indicative of a silicate composition similar to stony meteorites, with  $p_V$  normally in the range from 0.10 to 0.25.

S types dominate the inner main belt and the near-Earth population. S-type asteroids are therefore commonly associated with the most frequent meteorite type, the ordinary chondrites. However, the spectral features and albedos of the similar but less frequent *Q-type* asteroids fit those of ordinary chondrites much better. It is widely believed that S and Q-type asteroids are of identical bulk mineralogy, and that their surfaces age due to impacts by micro-meteorites and/or the solar wind (note that meteorites have lost their original surface during atmospheric entry), this process is called *space weathering*. In this picture, S and Q-type asteroids are respectively the old and young endmembers of a continuum; spacecraft imaging of the S-type asteroids Ida and Eros appears to support this idea (see Clark et al., 2002; Chapman, 2004a, for reviews). Recently, Lazzarin et al. (2006) found evidence that asteroids of other spectral types are also space weathered.

**X or EMP** Most remaining asteroids have rather featureless spectra at visible wavelengths, they are called X-type asteroids. There are three distinct groupings of X types differing in albedo:

**E** with high albedo ( $p_V > 0.3$ ), probably related to enstatite achondrite meteorites

**M** with moderate albedo ( $0.1 < p_V < 0.2$ ), some of which appear to be related to iron meteorites, but others appear to be non-metallic

**P** with very low albedo ( $p_V < 0.1$ ). P-type asteroids are believed to be composed of silicates very high in organic material, there are no known meteorite analogues. Together with the equally dark D-type asteroids (not listed here), P types are very abundant among the Jupiter Trojans. Some D and P-type asteroids in the near-Earth population are believed to be extinct cometary nuclei (depending on their orbital properties).

For X types, an albedo determination is particularly diagnostic of mineralogical composition. The study of composition and possible subtle spectral features of X-type asteroids is a very active area of research.

### 1.5.3 Spin rate

Asteroid spin rates differ significantly from object to object, from only a few minutes up to several weeks. The rotation states of MBAs are mostly determined from mutual collisions: The observed spin rates of MBAs larger than 50 km in diameter follow a Maxwellian distribution as predicted by this model, with a mean rotation period around 10 h (Harris and Pravec, 2006). Smaller asteroids deviate, increasingly so with decreasing size, from a Maxwellian distribution. In comparison, both very low and very high rotation rates are over-represented, indicating the presence of an effect capable of spinning small asteroids up or down. The YORP effect is widely believed to be responsible for this (Harris and Pravec, 2006).

There is an intriguing dichotomy in asteroid spin rates: While the periods of all known asteroid larger than 1 km in diameter are larger than 2.2 h, most smaller objects spin significantly faster, at spin rates of only a few minutes in extreme cases. This is widely seen as indicative of their internal structure (see sect. 1.5.5).

#### 1.5.4 Shape and spin axis

The shape and spin axis of most asteroids are unknown. It must be kept in mind that asteroids are typically too small to be spatially resolved. There are two well-established techniques to determine physical models of asteroid shape and spin state from ground-based observations, namely from time-resolved photometric observations at optical wavelengths (see Kaasalainen et al., 2002) or from radar observations of their rotationally induced Doppler frequency shift (Ostro et al., 2002). Both methods typically require a large amount of input data taken at various aspect angles. Note that shape models obtained from the inversion of optical photometry are typically convex, concavities are virtually impossible to resolve using that technique.

Asteroid shapes found so far vary significantly: Larger MBAs are typically nearly spherical, although there are notable exceptions such as the “dog-bone shaped”  $217 \times 94 \times 81$  km asteroid (216) Kleopatra (Ostro et al., 2000). The shape diversity of smaller asteroids, most of which are expected to be collisional shards, is significantly larger. Upcoming asteroid discovery programs such as Pan-STARRS promise to provide an extensive database of well-calibrated optical photometric data, which will allow the shapes and spin states of at least several thousands of asteroids to be determined in the next decade (Ďurech et al., 2005).

#### 1.5.5 Internal structure—*are asteroids piles of rubble?*

The internal structure of asteroids is an important and very active area of research. In particular it is not clear whether asteroids have significant tensile strength or whether some (or most) are loose gravitational aggregates, called *rubble piles* (see Richardson et al., 2002, for a review). This is of particularly practical importance in the case of potential Earth impactors: Rubble piles may be significantly harder to deflect than monolithic objects.

**Surface morphology** The two asteroid rendezvous missions carried out so far revealed that Eros does not appear to be a rubble pile (Cheng, 2004a) while Itokawa does (Fujiwara et al., 2006). Flyby imaging revealed very large craters, comparable to the objects’ radii, on some asteroids (Gasptra, Ida, and Mathilde) and on Mars’ satellite Phobos, presumably a captured asteroid. Those large craters are largely seen as indicative of a very weak, rubble-pile-like internal structure (see, e.g., Chapman, 2002; Cheng, 2004a, and references therein) because monolithic



bodies would be expected to be disrupted by shock waves such as those generated during the crater-forming impacts. Weak, porous bodies dissipate shock waves efficiently and can therefore sustain much larger impacts (Holsapple et al., 2002). This is supported by the presence of adjacent and undisturbed large craters on Mathilde; on a solid target, the formation of the later crater would have significantly affected the former.

**Mass density** Inferences on internal structure can be made from the mass density, which is known for a small set of asteroids consisting of spacecraft targets, some binary systems (see sect. 1.5.6), and a few asteroids which made recent close encounters with other asteroids (Hilton, 2002). While the bulk mass densities of the largest MBAs above 500 km in diameter match those of analogue meteorites very well, smaller objects are significantly under-dense. There is a cluster of objects, including Eros, with macroporosities around 20 % (i.e. 20 % of the volume is apparently void) which are believed to contain major cracks formed by shattering through sub-catastrophic impacts. Other objects display much higher macroporosities, beyond 50 % in extreme cases; these objects must contain major voids and are widely believed to be rubble piles (Mathilde falls into this category, which is consistent with its craters mentioned above) (see Britt et al., 2002, for a review).

It is worth noting that the uncertainty in mass density is typically dominated by the diameter uncertainty (see Merline et al., 2002; Richardson and Walsh, 2006).

**Spin rate** Further information can be potentially obtained from the observed dichotomy in asteroid spin rates (see sect. 1.5.3): As was first noted by Harris (1996), the apparent “spin barrier” around 2.2 h coincides with the spin rate at which the centrifugal force at the equator of a spherical body equals gravity. Rubble piles at faster spin rates would therefore disrupt, the conspicuous lack of such fast rotators larger than 1 km appears to indicate that most, if not all, of them are rubble piles. Small fast rotators, on the other hand, are held together by tensile strength and are expected to be monolithic.

Both conclusions have recently been challenged by Holsapple (2007) who argues that for bodies larger than some 10 km in diameter, tensile strength is negligible relative to gravity. As a result, such asteroids are subject to the quoted spin barrier even if they possess significant tensile strength. Holsapple estimated the tensile strength required to stabilize known small fast rotators to be on the order of only 10–100 kPa, “the strength of moist sand” in the words of the author.

### 1.5.6 Binarities

An intriguing asteroid sub-population is that of the binary asteroids, i.e. asteroids with a gravitationally bound satellite. The first asteroid satellite, Dactyl, was found orbiting the MBA (243) Ida through imaging from the *Galileo* spacecraft (Belton et al., 1996). Since then, some 70 binary asteroid systems have been discovered, using different observational techniques. Their orbits range from near-Earth space out into the trans-Neptunian region, with primary body diameters between just a few kilometers and several hundred (Richardson and Walsh, 2006; Noll, 2006).

The mass, which for asteroids is only rarely known (see Hilton, 2002), can be calculated for binary systems from Newton's form of Kepler's Third Law if the mutual orbit is well constrained.

The total angular momentum of most small NEA binaries is just above the critical limit at which a single body of equal mass would disrupt. This indicates that they were formed from a parent body which was spun up (e.g. through the YORP effect), ultimately leading to its fission into a binary system (Harris and Pravec, 2006). This is seen as an indication for their being rubble piles (see sect. 1.5.5), which is consistent with the low lightcurve amplitude of most binaries.

### 1.5.7 Regolith

Large atmosphereless bodies such as Mars, Mercury, or our Moon are known to be covered with a thick layer of regolith, which formed from retained impact ejecta. Large asteroids are known to display at least some regolith on their surfaces, smaller objects are known to be increasingly depleted in fine dust grains (see, e.g., Dollfus et al., 1989).<sup>9</sup> This latter finding was explained with the low asteroid gravity which allows fine impact ejecta (with higher average thermal velocities) to escape. Asteroids below a certain threshold size were thus expected to be basically regolith free, the threshold diameter was estimated to be between 10 and 70 km (see Scheeres et al., 2002, for a review). This was consistent with the findings of Lebofsky et al. (1979) and Veeder et al. (1989), who indirectly estimated the thermal inertia (see sect. 1.5.8) of a number of small NEAs to be very high, indicating a lack of thermally insulating regolith on their surfaces.

To the big surprise of the asteroid community, however, spacecraft imaging in

---

<sup>9</sup> Throughout this thesis, regolith is loosely defined as a layer of particulate material covering the surface or parts of it.

1991 (see sect. 1.1) revealed indications for a substantial regolith layer on the MBA (951) Gaspra with an effective diameter of only 12 km. The NEA (433) Eros, around 17 km in diameter, was unambiguously seen to be thickly covered with regolith, although an intriguingly large number of boulders are present on its surface. Even the small NEA (25143) Itokawa (effective diameter around 320 m) is not entirely regolith free: recent spacecraft imaging showed a thought-provoking surface dichotomy between boulder-strewn surface patches, apparently devoid of powdered material, and very flat, regolith-dominated regions (see Fig. 1.1 on p. 2).

While the origin of regolith on asteroids is far from being completely understood, it is plausible that the regolith found on relatively small asteroids indicates a weak surface structure, i.e. low material strength and/or high porosity (see, e.g., Asphaug et al., 2002; Chapman, 2002; Holsapple et al., 2002; Scheeres et al., 2002). In this case, crater formation is dominated by gravity rather than material strength, which reduces ejecta velocities and enables the gravitational retention of a non-negligible fraction thereof. This conforms with first results from the *Deep Impact* mission (A’Hearn et al., 2005), where a 370 kg projectile hit the nucleus of comet 9P/Tempel 1 at a relative velocity of 10.3 km/s—apparently a significant fraction of the ejected dust was very slow and later reaccumulated, indicative of a very low material strength of the nucleus. We caution, however, that the formation and later dynamics of ejecta is likely to be very different among comets and asteroids.

No detailed spacecraft imaging is available for asteroids between 0.32 km (Itokawa) and 12 km (Gaspra) in diameter; it is therefore unclear if they display regolith or not. In particular it is unclear whether there is a clear transition size above which asteroids are fully covered with regolith, while smaller objects are not. In the light of the previous paragraph, studies of asteroid regolith coverage may allow conclusions to be drawn on the elusive but important material strength and may further our understanding of regolith formation through impact processes.

### 1.5.8 Thermal inertia

Thermal inertia is a measure of the resistance to changes in surface temperature: The surface of a body with low thermal inertia heats up or cools down readily, while bodies with high thermal inertia tend to keep their surface temperature for longer (see sect. 2.2.2 for a more detailed discussion).

*Thermal inertia governs the important Yarkovsky and YORP effects* (see sect.

## 1 Introduction

1.3); thermal inertia estimates are crucial for model calculations of both. Thermal inertia also determines the temperature environment in which lander missions (see, e.g., Binzel et al., 2003, for some considerations) have to operate: Low thermal inertia causes harsh temperature contrasts between the day and the night side, while in the case of high thermal inertia the diurnal temperature profile is much smoother. Furthermore, thermal inertia is a very sensitive indicator for the presence or absence of regolith on the surface (see sect. 1.5.7): The thermal inertia of lunar regolith is some 50 times lower than that of bare rock, which in turn is nearly an order of magnitude below that of metal (see table 3.1 on p. 58). This is widely used in planetary science; several Mars orbiters, e.g., carried temperature sensitive instruments in order to derive global thermal-inertia maps by means of which exposed bedrock can be distinguished from regolith (see, e.g., Christensen et al., 2003; Putzig et al., 2005, and references therein).

Little is known so far about the thermal inertia of asteroids, virtually nothing is known about the thermal inertia of small asteroids including NEAs. Ground-based determinations of asteroid thermal inertia are challenging, both in terms of observing and modeling: Extensive spectrophotometric or spectroscopic observations in the difficult mid-infrared wavelength range ( $\sim 5\text{--}35\ \mu\text{m}$ ) are needed (see sect. 2.3). Such observations are hampered by the large atmospheric opacity throughout most of this wavelength range, combined with a large level of background radiation stemming from the atmosphere, clouds, and the telescope itself which emits thermal radiation peaking at a wavelength around  $10\ \mu\text{m}$ . On the modeling side, difficulties arise because crucial parameters such as the object's shape and spin state are typically not known. Furthermore, sufficiently detailed thermophysical models had so far only been tested for application to large MBAs, which differ from small NEAs in many important ways (see Harris and Lagerros, 2002, for a review and chapter 3 for a detailed discussion).

It was realized already in the 1970s that the typical thermal inertia of large asteroids must be small, comparable to that of the Moon (see, e.g., Morrison, 1977, for a review). However, no quantitative results were available, with the notable exception of (433) Eros (Lebofsky and Rieke, 1979, based on a very approximate shape model) and (1) Ceres and (2) Pallas (Spencer et al., 1989). The first large-scale thermal-inertia study was by Müller and Lagerros (1998) who quantitatively determined the thermal inertia of 5 large MBAs.

There has been some controversy about the typical thermal inertia of NEAs, which had not been measured directly so far. Lebofsky et al. (1978, 1979) and

Veeder et al. (1989) found indirect evidence that a significant fraction of NEAs should have a very high thermal inertia indicative of a surface consisting of bare rock. Delbo' et al. (2003), on the other hand, performed a thermal spectrophotometric survey of NEAs and stated that the majority of their targets must possess a thermally insulating layer of regolith. Note that the thermal inertia of small asteroids is particularly relevant since they are substantially influenced by the Yarkovsky effect (see sect. 1.3) which is governed by thermal inertia.

## 1.6 Scope of this work

*The primary aim of this work is to augment the number of asteroids with known thermal inertia.* Emphasis is put on NEAs for which practically no reliable information is available so far. We have also determined the size and albedo of two asteroid targets of upcoming spacecraft visits.

The following questions are addressed:

- What is the typical thermal inertia of NEAs?
- What can be learned about their regolith coverage?
- Does thermal inertia depend on size, as might be expected from models of regolith retention?
- What is the size and albedo of our targets, and how can we constrain their surface mineralogy?

This requires extensive observations of the thermal emission of our targets in the mid-infrared wavelength range ( $\sim 5\text{--}35\ \mu\text{m}$ ), combined with observations of the reflected sunlight and a suitable model of the thermal emission.

An adequate thermophysical model for NEAs has been developed and tested (see chapter 3). Previously available models of NEA thermal emission are not sufficiently detailed for the quantitative determination of thermal inertia, while available thermophysical models for atmosphereless bodies (on which the model described herein is based) were neither designed nor tested for application to NEAs.

Observations were made with the NASA Infrared Telescope Facility on Mauna Kea / Hawai'i (chapter 4) and the Spitzer Space Telescope (chapter 5).

We present detailed studies of individual objects rather than a general survey; our results for individual asteroids are presented in chapter 6. Nevertheless, our

## *1 Introduction*

results allow the first firm conclusions to be drawn on the NEA distribution in thermal inertia. These and other results are discussed in chapter 7.

In the final chapter 8 our main conclusions are summarized, possible future work is discussed in chapter 9.